Tarzamni, Hadi; Esmaeelnia, Farhad Panahandeh; Tahami, Farzad; Fotuhi-Firuzabad, Mahmud; Tohidi, Sajjad; Dehghanian, Payman; Lehtonen, Matti

Thermal analysis of non-isolated conventional PWM-based DC-DC converters with reliability consideration

Published in:
IET Power Electronics

DOI:
10.1049/pel2.12037

Published: 01/02/2021

Document Version
Publisher's PDF, also known as Version of record

Received: 24 May 2020 | Revised: 23 August 2020 | Accepted: 26 August 2020

IET Power Electronics

DOI: 10.1049/pel2.12037

The Institution of Engineering and Technology WILEY

ORIGINAL RESEARCH PAPER

Thermal analysis of non-isolated conventional PWM-based DC–DC converters with reliability consideration

Hadi Tarzamni[1] | **Farhad Panahandeh Esmaeelnia**[2] | **Farzad Tahami**[1] | **Mahmud Fotuhi-Firuzabad**[1] | **Sajjad Tohidi**[2] | **Payman Dehghanian**[3] | **Matti Lehtonen**[4]

[1] Electrical Engineering Department, Sharif University of Technology, Tehran, Iran

[2] Faculty of Electrical and Computer Engineering, University of Tabriz, Tabriz, Iran

[3] Department of Electrical and Computer Engineering, George Washington University, Washington, DC, USA

[4] Department of Electrical Engineering and Automation, Aalto University, Espoo, Finland

Correspondence
Farzad Tahami, Electrical Engineering Department, Sharif University of Technology, Tehran, Iran.
Email: tahami@sharif.edu

Abstract

This paper proposes analytics for reliability assessment of non-isolated conventional pulse width modulation DC-DC (NIDC-DC) converters. This class of converters consists of conventional Buck, Boost, Buck–Boost, Cuk, Sepic and Zeta topologies. The proposed analytics are founded based on the Markov process principles and can effectively capture the effects of duty cycle, input voltage, output power, voltage gain, components characteristics and aging on the overall reliability performance and mean time to failure of the NIDC-DC converters. Furthermore, the suggested framework takes both continuous and discontinuous conduction modes of each converter into account, with which the open and short circuit faults in the components are analysed. As an important outcome, the most reliable operation region of the NIDC-DC converters are obtained with respect to different operational parameters, which is useful in design procedure. Eventually, extensive thermal experiments with an appropriate reflection of reliability metric are conducted to measure the components' temperatures and verify their performance in different operating conditions.

1 | INTRODUCTION

With the rapid advancement and wide deployment of power electronic infrastructure in the electric industry, comprehensive analysis of power electronic converters from different aspects has attracted significant research and development [1–3]. The reliability assessment of the power electronic interfaces is attributed an intensified priority [4–6], particularly highlighted in mission-critical and high-cost applications [7], since it helps reveal their performance under different fault conditions in various applications [8].

Among various classes of power electronic converters, DC–DC converters are widely applied in several critical power electronic interfaces, such as grid-edge renewable energy systems, electrical vehicles, aircrafts, and home appliances. Maloperation or performance degradation of DC–DC converters in different applications unleash significant consequences [9]. Reference [10] took a step forward in a promising direction to evaluate the effects of characteristic changes in each component of such converters on the operating point of other components and overall reliability, thereby resulting in a significant reduction in maintenance costs. While centred on conventional Boost converter in a closed-loop control operation, the analyses in [10] are generic enough to be applied to other types of power converters. It has been demonstrated in [10] that (i) an increase in the modelled series resistance of the main switch or in the output capacitor would result in a degradation of the converter's overall reliability performance, and (ii) the variation in the converter's capacitor reveals a complicated, and at times hard to characterize, impacts on the converter's reliability. Optimal design of the LC filter in the conventional Buck converter is approached in [11], where the reliability metrics as well as other operational parameters such as voltage and current ripples, power density and costs are co-optimized. Furthermore, the relationship between the filter capacitor lifetime and its electro-thermal stress is characterized in [11] taking into account different size and classes of filter capacitance and inductance. Reliability performance of a three-phase soft switching interleaved Boost

converter is evaluated in [12] and compared with hard switching interleaved Boost converter and interleaved configurations in [13] and [14]. Soft switching is achieved in [12] with no need to consider any additional component, which in turn, improves its reliability performance. Reference [15] focuses on the reliability evaluation of an interleaved pulse width modulation (PWM) Boost converter in both single stage and interleaved operating modes. With the main goal of optimizing the number of interleaved Boost converters through a cost-reliability trade-off, the assessments in [15] are presented for two and three interleaved Boost converters connected to photovoltaic input sources, where comparisons between interleaved operating condition (where all parallel converters operate) and semi-redundant operating condition (where one converter operates and the others are in standby) demonstrated a higher reliability performance in the former. In [16], reliability analysis is presented on single stage and interleaved conventional Boost converters, where Markov models are employed in the latter to investigate the reliability performance in two distinct scenarios of half and full nominal power operation modes for one stage following a failure in the other. It was concluded in [16] that the two-stage interleaved Boost converter with half power operation mode, although requiring additional components, is attributed a higher reliability than the conventional single stage Boost converter. Reliability analysis of the multi-phase DC–DC converters in photovoltaic energy conversion systems are evaluated in [17], where (i) the role of additional parallel stages on the components' failure rates and the system's overall reliability performance is extensively investigated and (ii) a trade-off is achieved between the capacitor voltage ripples and converter's overall reliability performance via apt sizing of the system capacitors. Reliability of a full soft switching Boost converter is compared with its interleaved topology and hard switching conventional PWM Boost converter in [18] under open circuit (OC) fault scenarios. In case of a single stage soft switching converter facing an OC fault in any of its auxiliary resonant components, the converter continues to operate in hard switching mode with higher switching loss. In the case where the OC fault occurs on the main components of the Boost converter, the converter would transition to an absorbing state (total failure). Extensive analysis in [18] demonstrated that the interleaved soft switching two-phase converter is attributed the highest reliability performance. In [19], a four-step fault tolerant full bridge DC–DC converter with phase shift control is presented for the main sake of improved reliability and its performance is analysed under OC fault instances. Fault diagnosis is achieved through an additional winding to the primary side of the transformer: if an OC fault occurs in any primary-side switch, the fault detection method operates and the controlling system triggers an active phase shift to tolerate the fault. A single switch DC–DC converter with fault tolerant capability and higher reliability performance is presented in [20], where the reliability assessments are centred on both short circuit (SC) and OC faults. In [21], reliability of isolated multi-switch DC–DC converters is analysed with main focus on their self-embedded fault tolerance, where various experimental tests are performed to evaluate the impact of different faults on the converters' total operation.

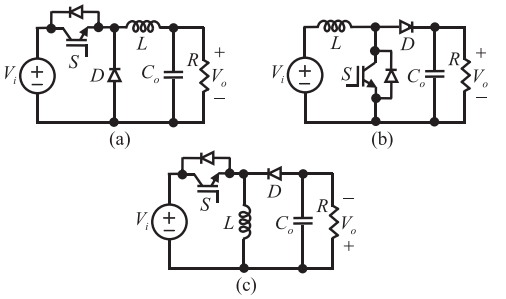

FIGURE 1 NIDC-DC converter topologies with two passive components: (a) Buck; (b) Boost; (c) Buck–Boost

This paper offers advanced analytics for reliability evaluation of non-isolated conventional PWM DC-DC (NIDC-DC) converters. Different from the past literature—that generally focus on Buck and Boost converters solely in particular operating points and with a restricted selection of parameters, the proposed analytics are comprehensive in that inclusively capture various operating conditions and critical parameters (e.g., duty cycle, input voltage, output power, voltage gain, components characteristics and aging) of all different classes of NIDC-DC converters, including the Buck, Boost, Buck–Boost, Cuk, Sepic and Zeta topologies (see Figures 1 and 2). The suggested framework encompasses both continues and discontinuous conduction modes (CCM and DCM) for each converter and takes into account both the SC and OC fault types.

The rest of the paper is organized as follows. Section 2 provides the theoretical background on the Markov model and its applications in reliability evaluations. Section 3 presents the reliability evaluation of different classes of NIDC-DC converters with sub-sections focusing on the contributing parameters and operating conditions. Section 4 is devoted to the mean time to failure (MTTF) assessments of the NIDC-DC converters followed by the experimental verifications and thermal tests in Section 5. Finally, Section 6 concludes the paper.

2 | MARKOV MODELS: FUNDAMENTAL PRINCIPLES

Continuous Markov process is one very popular approach to probabilistically solve many classes of problems, particularly reliability assessments of systems and individual equipment, in different engineering disciplines. In this paper, Markov process is employed to formulate the reliability of six classes of NIDC-DC converters (see Figures 1 and 2), demonstrated in Figure 3. According to Figure 3, these converters are modelled through two distinct operating states of healthy (initial) and failure (absorbing). Transition from healthy to absorbing state is realized in case of any SC or OC fault in the converter elements. According to the Markov model presented in Figure 3, reliability performance of NIDC-DC converters can be formulated as a function of time as presented in Equation (1):

$$R(t) = P_1(t) \tag{1}$$

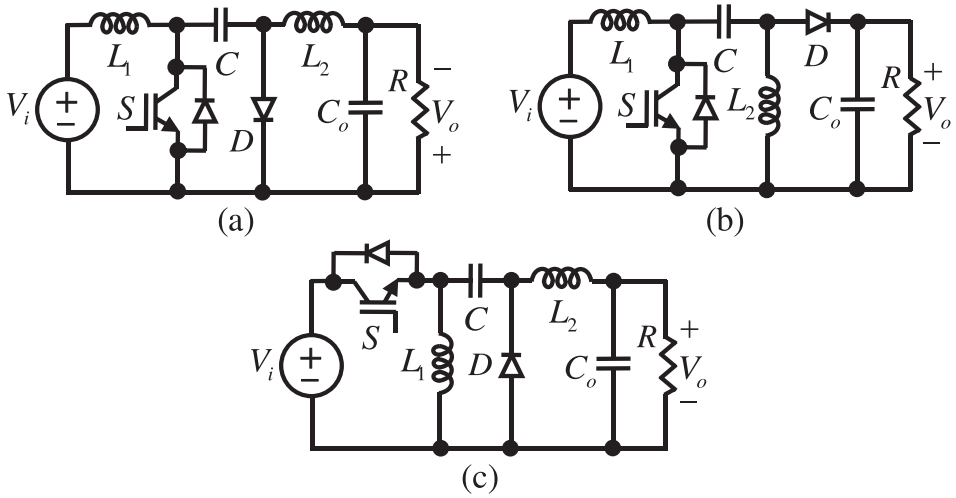

FIGURE 2 NIDC-DC converter topologies with four passive components: (a) Cuk; (b) Sepic; and (c) Zeta

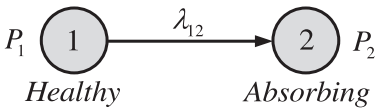

FIGURE 3 Markov model for the NIDC-DC converters

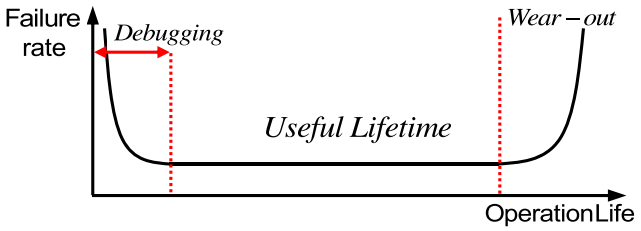

FIGURE 4 Failure rate of a component in its operation life time [24]

where, $P_1(t)$ is the probability of residing in the healthy operating state, which in other words, reflect the overall reliability performance of the NIDC-DC converters and is assessed through the following state space equation.

$$d/dt\begin{bmatrix}P_1(t) & P_2(t)\end{bmatrix} = \begin{bmatrix}P_1(t) & P_2(t)\end{bmatrix}\begin{bmatrix}-\lambda_{12} & \lambda_{12}\\ 0 & 0\end{bmatrix} \quad (2)$$

where, λ_{12} is the failure rate of the converters reflecting the possible transition from the healthy to the absorbing operating state. $P_2(t)$ is the absorbing state probability, where the summation $P_1(t) + P_2(t) = 1$ always holds.

As the leading cause of failures in NIDC-DC converters, SC and OC faults are taken into account to characterize the failure rate λ_{12} for the Buck, Boost, and Buck–Boost classes of converters in Equation (3a) and for the Cuk, Sepic, and Zeta converters in Equation (3b).

$$\lambda_{12} = \lambda_S + \lambda_{GD} + \lambda_D + \lambda_L + \lambda_{Co} \quad (3a)$$

$$\lambda_{12} = \lambda_S + \lambda_{GD} + \lambda_D + \lambda_{L1} + \lambda_{L2} + \lambda_C + \lambda_{Co} \quad (3b)$$

where, λ_S, λ_{GD}, λ_D, λ_L and λ_{Co} are, respectively, the failure rates corresponding to the switch, gate driver, diode, inductor and output capacitor elements in the Buck, Boost and Buck–Boost converters when both SC and OC faults are considered. Furthermore, since Cuk, Sepic and Zeta classes of converters are implemented through one additional capacitor and inductor elements compared to the others, the associated Markov model would incorporate two additional component failure rates. Note that, the effects of conduction and switching losses are considered in λ_S and λ_D. The component failure rates are primarily driven by several factors such as quality, material, voltage stress, environmental conditions, temperature and power loss, the contributions of which are formerly assessed in the case of MIL-HDBK-217 in [22, 23]. The failure rate of each component is considered constant, if and only if the component is operating within its useful life time, as illustratively demonstrated in the failure rate curve—commonly known as the bath-tub curve—in Figure 4. According to Figure 4, each component can reside in three operating intervals in its life time, designated as the debugging, useful life, and wear-out intervals. As in the case of many engineering applications, including the power electronic converters, the assumption on the components operating in their useful life interval is acceptable since this span is typically long in practice [24].

Assuming the initial operating state to be the healthy state, the initial condition in Equation (2) is expressed as follows:

$$\begin{bmatrix}P_1(0) & P_2(0)\end{bmatrix} = \begin{bmatrix}1 & 0\end{bmatrix} \quad (4)$$

Thus, according to Equation (4), $P_1(t)$ can be assessed in Equation (5).

$$P_1(t) = e^{-\lambda_{12}t} \quad (5)$$

TABLE 1 Design parameters of each converter

Converter	L_1	L_2	C	C_o	D_B
Buck	1.5 mH	–	–	100 uF	0.4
Boost	0.5 mH	–	–	250 uF	0.38
Buck–Boost	1.2 mH	–	–	200 uF	0.31
Cuk, Sepic, Zeta	1.5 mH	1 mH	25 uF	200 uF	0.51

Eventually, the MTTF index of reliability is defined as in Equation (6).

$$\text{MTTF} = \int_{t=0}^{\infty} P_1(t)\,dt = 1/\lambda_{12} \tag{6}$$

3 | RELIABILITY EVALUATION OF NIDC-DC CONVERTERS

Several critical factors and operating conditions are conjoined in the proposed analytics to derive the reliability behaviour of the six classes of NIDC-DC converters. Expressly, these parameters include the duty cycle (D), input voltage (V_i), output power (P_o), voltage gain (G) and aging (t) as well as variations in components characteristics. The reliability performance indicators, based on the steady-state power-loss analytics of [24], are evaluated and comprehensively compared under both DCM and CCM. Borrowed from [25], the NIDC-DC converters are assumed to be designed with a switching frequency of 20 kHz, output load of 100 Ω and minimum and maximum acceptable duty cycles of $D_{min} = 0.1$ and $D_{max} = 0.9$, respectively. The design parameters for each converter under the same operating conditions is presented in Table 1, where D_B reflects the boundary duty cycle differentiating the DCM and CCM. In addition, sample semiconductor devices are assumed for the switch and diode, where the switch is modelled with a forward ON voltage drop of 1 V and drain-source ON-resistance of 0.049 Ω, while these parameters take 1.5 V and 0.023 Ω values for the diode, respectively.

In this section, the formulated failure rates of components are only presented for CCM Buck–Boost converter. In addition, the resulted plots of converters with similar characteristics are not demonstrated.

3.1 | Effects of duty cycle and aging on reliability

In this section, we assess the reliability performance of the NIDC-DC converters in both DCM and CCM where the parameters D and t are assumed variables, the output power is considered 100 W and as the sample results, the components' failure rates of Buck–Boost converter under CCM operating mode are evaluated as follows:

$$\lambda_{Co}(D) = 0.02 \tag{7}$$

$$\lambda_L(D) = 5\times10^{-5}\exp\left(-1276\left(\frac{1}{298+\frac{44}{(1-D)^2}}-\frac{1}{298}\right)\right) \tag{8}$$

$$\lambda_D(D) = 0.0038\left(\frac{1}{6D}\right)^{2.43}\exp\left(-3091\left(\frac{1}{413.2+\frac{1.47}{1-D}}-\frac{1}{298}\right)\right) \tag{9}$$

$$\lambda_S(D) = 0.48\exp\left(-1925\left(\frac{1}{298+\frac{40.7D}{1-D}+\frac{2D}{(1-D)^2}+\frac{2.12}{D^2}}-\frac{1}{298}\right)\right) \tag{10}$$

$$\lambda_{GD}(D) = 72\times10^{-6} \tag{11}$$

According to Equations (3), (5) and the calculated components' failure rates of each converter, Figures 5, 6 and 7 demonstrate the three-dimensional plots of how the NIDC-DC converters' reliability performance changes as a function of D and t. One can see generically for all different classes of the NIDC-DC converters that the reliability performance degrades as time elapses, but in a different rate. The case of CCM Cuk converter has shown the highest reliability degradation with respect to the aging factor, while it is the lowest in the case of the DCM Buck converter, particularly for duty cycles around D_B. In order to precisely compare the effects of D and t on the systems' reliability performance, Figure 8 illustrates that the Buck–Boost converter is attributed an acceptably high reliability performance in a wide operational region of $0.2 < D < 0.75$.

Reliability performance comparison of different NIDC-DC converter topologies with respect to D is illustrated in Figure 9(a,b), respectively under the DCM and CCM operating modes. One can see, from Figure 9 that the reliability performance of different converter topologies—except that of the Boost topology—generally increases from D_{min} to a maximum value under DCM operation mode. In other words, the maximum reliability point is achieved for the Buck, Buck–Boost, Cuk, Sepic and Zeta converter topologies in the DCM operation region; however, reliability reduces from D_{min} to D_{max} in the Boost converter. Under the CCM operation mode, the converter reliability performance is inversely proportional to the duty cycle, which is due to the higher switch conduction losses when the duty cycle ranges around D_{max}. Any increase in duty cycle results in the highest and lowest impact on the reliability degradation of the Cuk and Buck converters, respectively. Moreover, the Cuk converter has shown the least reliability performance under a CCM operation as it contains additional number of components. All the NIDC-DC converter topologies (except the Buck converter) are in general attributed a very low reliability performance in $D > 0.75$ and $t > 0.9\times10^6$h. Additionally, it is observed that the Cuk, Sepic, and Zeta

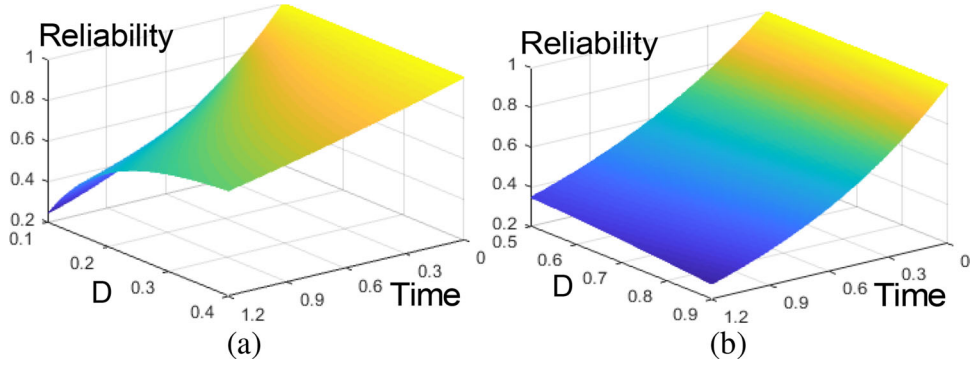

FIGURE 5 Reliability performance of the Buck converter with respect to D and t (h×10^6): (a) DCM; (b) CCM

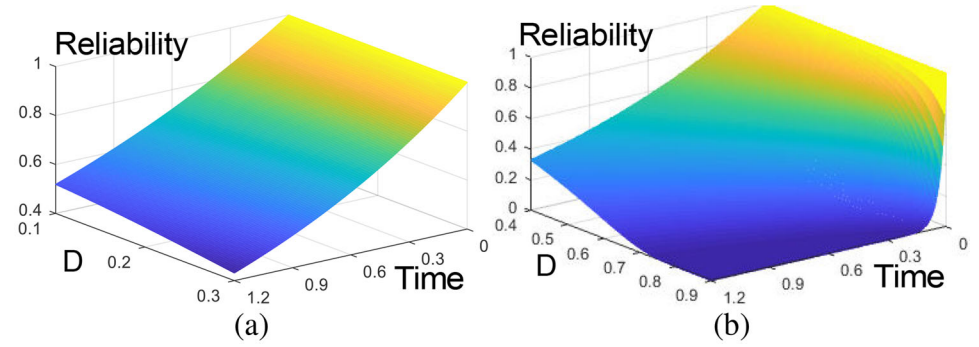

FIGURE 6 Reliability performance of the Boost converter with respect to D and t (h×10^6): (a) DCM; (b) CCM

converter topologies represent an approximately similar reliability performance.

Reliability of the converters are calculated with four decimal digits. In Figure 10, the duty cycle captured at a maximum reliability performance is presented in different time durations for Cuk converter, where a range of duty cycle variations in each time step is realized when the maximum reliability performance is achieved. It is clear that the calculations with more decimal digits lead to a narrower range, and the duty cycle converges to an optimal value as time elapses.

In order to evaluate the effect of D on the failure rates of converter components, Figure 11 demonstrates the sensitivity of λ_S, λ_D and λ_L with respect to D under both CCM and DCM operating modes. The sensitivities are evaluated through

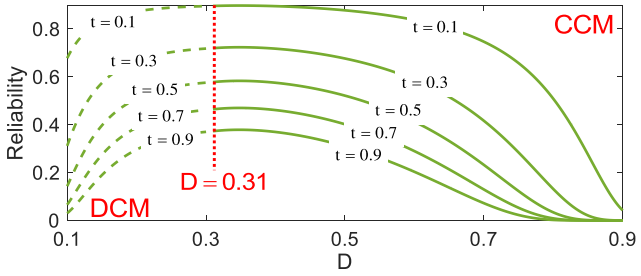

FIGURE 8 Reliability performance of the Buck–Boost converter with respect to D in different t (h×10^6)

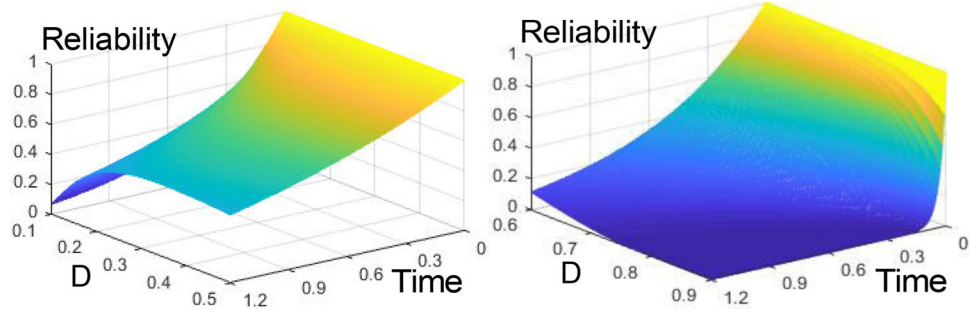

FIGURE 7 Reliability performance of the Cuk converter with respect to D and t (h×10^6): (a) DCM; (b) CCM

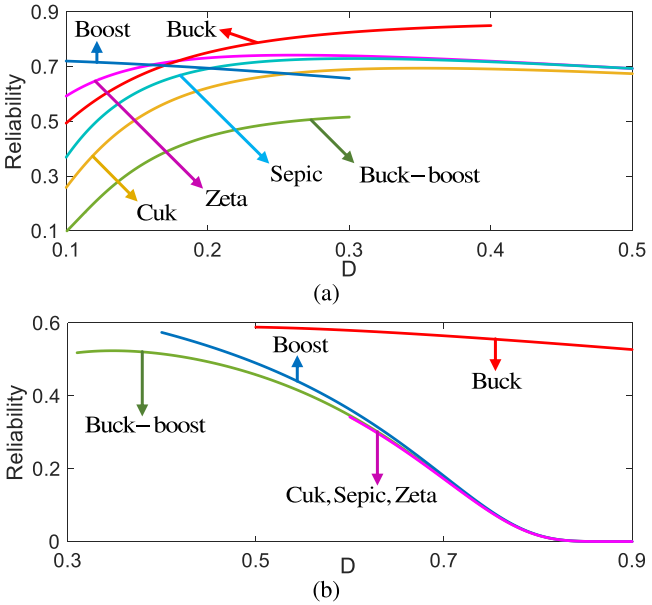

FIGURE 9 Reliability performance comparison of NIDC-DC converter topologies with respect to D at $t = 0.6 \times 10^6$ h: (a) DCM and (b) CCM

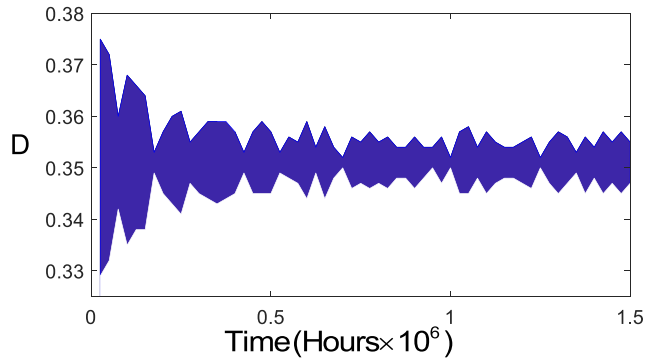

FIGURE 10 Duty cycle in the maximum reliability region in the Cuk converter

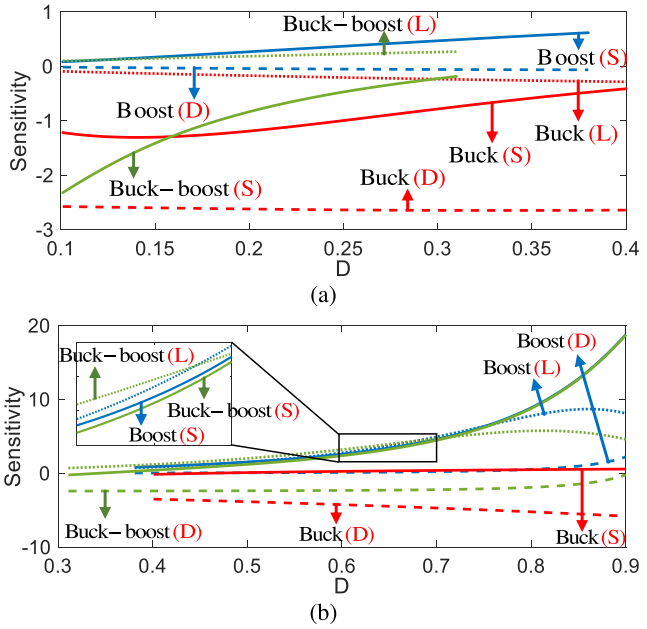

FIGURE 11 Components' failure rate sensitivity comparison of NIDC-DC converter topologies with respect to duty cycle at $t = 0.6 \times 10^6$ h (S, D and L represent switch, diode and inductor, respectively): (a) DCM, (b) CCM

$(d\lambda(D)/dD).(D/\lambda(D))$, where $\lambda(D)$ is replaced by $\lambda_S(D)$, $\lambda_D(D)$ and $\lambda_L(D)$ for each component. As presented in Figure 11(a), the components failure rates of the DCM Boost converter are achieved positive, reflecting the fact that the reliability performance degrades as D increases—similar to observations made in Figure 6(a). However, the summation over the failure rate sensitivities are evaluated negative for all other converter topologies, leading to improvements in the reliability performance as D increases—verifying the observations in Figure 5(a) and 7(a). Furthermore, the diodes of Buck and Boost converters are the most and the least sensitive components in D variations of DCM, respectively. One can see in Figure 11(b) that $\lambda_S(D)$ of CCM Boost converter reveals the highest sensitivity, particularly when $D > 0.75$, manifesting the reliability performance degradation to very low values of this converter in $D > 0.7$. In the case of CCM Buck–Boost converter, $\lambda_D(D)$ and $\lambda_S(D)$show higher sensitivity in $D < 0.6$ and $D > 0.6$, respectively (when considering the absolute values). This is primarily observed due to the time length associated with the switch and diode conduction intervals, which rises and falls, respectively, as D increases.

3.2 | Effects of input voltage and aging on reliability

In this section, the effect of V_i variations on the reliability performance of multiple classes of NIDC-DC converter topologies in different t is investigated under both DCM and CCM operating modes. Duty cycles are assumed to be 1/3 and 2/3, respectively for the DCM and CCM scenarios. The components failure rates corresponding to the CCM Buck–Boost converter are determined as follows.

$$\lambda_{Co}(V_i) = 0.013\left(\left(4.096 \times 10^{-6} V_i^3\right) + 1\right) \tag{12}$$

$$\lambda_L(V_i) = 5 \times 10^{-5} \exp\left(-1276\left(\frac{1}{298 + 0.16V_i^2} - \frac{1}{298}\right)\right) \tag{13}$$

$$\lambda_D(V_i) = 0.0038\left(\frac{V_i}{198.02}\right)^{2.43} \times \exp\left(-3091\left(\frac{1}{298 + 2.18V_i + 1.8 \times 10^{-3} V_i^2} - \frac{1}{298}\right)\right) \tag{14}$$

$$\lambda_S(V_i) = 0.48$$

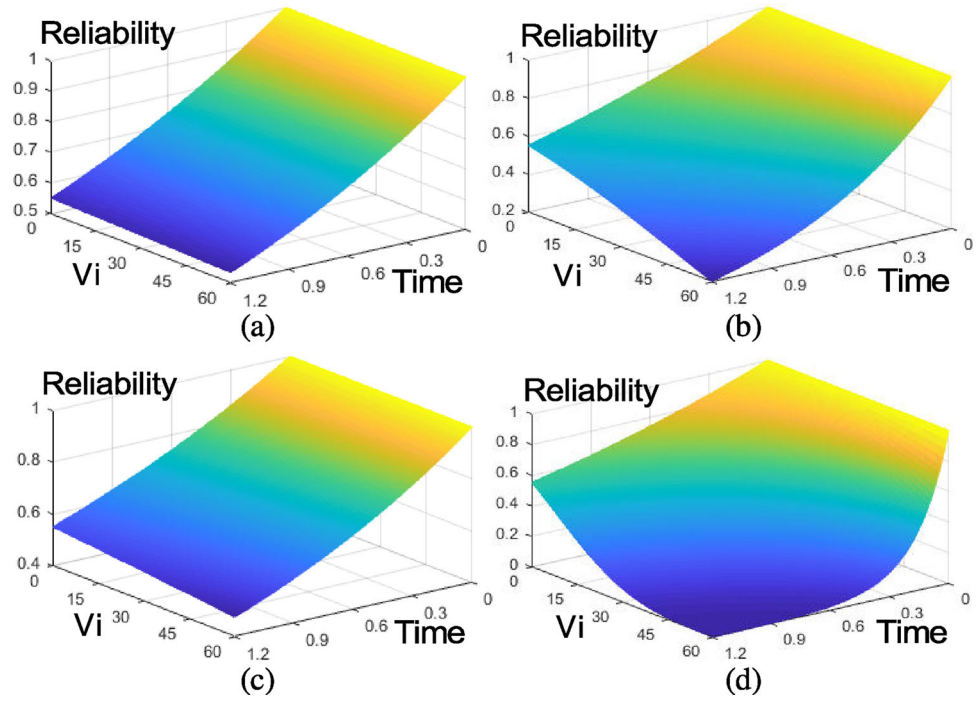

FIGURE 12 Reliability performance of the NIDC-DC converter topologies with respect to V_i (V) and t (h×10^6): (a) DCM Buck; (b) DCM Boost; (c) CCM Buck; and (d) CCM Boost

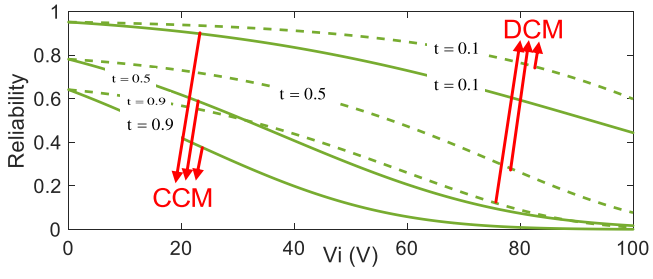

FIGURE 13 Reliability performance of the Buck–Boost converter with respect to V_i at different t (h×10^6) values

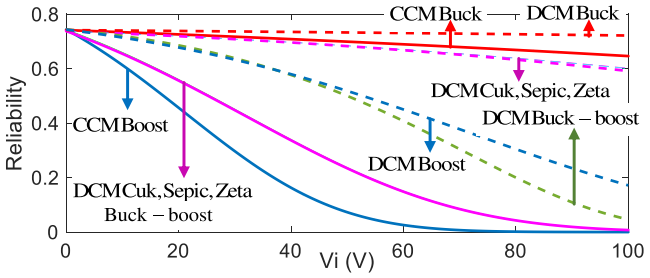

FIGURE 14 Reliability performance comparison of different NIDC-DC converter topologies with respect to V_i at $t = 0.6 \times 10^6$ h

$$\times \exp\left(-1925\left(\frac{1}{298 + 1.63V_i + 6.68 \times 10^{-3}V_i^2} - \frac{1}{298}\right)\right) \tag{15}$$

$$\lambda_{GD}(V_i) = 72 \times 10^{-6} \tag{16}$$

The three-dimensional plots on the reliability performance of the Buck and Boost converters with respect to variations in V_i and t are illustrated in Figure 12. Figure 13 also comparatively illustrates the reliability performance of the DCM and CCM Buck–Boost converters for different selections of t. Furthermore, the reliability of NIDC-DC converters in both DCM and CCM are compared in Figure 14 at $t = 0.6 \times 10^6$ h. One can realize from these illustrations that, in all NIDC-DC converter topologies, the DCM operation offers a higher reliability performance than the CCM, primarily due to the higher conduction losses of switches in the latter. Furthermore, the higher the V_i, the higher the voltage stress, resulting in an intensified switching loss and accordingly, lower system reliability performance. The other interesting observation is the rate at which the reliability performance degrades as V_i increases, where a higher rate of reliability degradation is attributed to the CCM operation modes. Comparing different classes of NIDC-DC converters, the DCM and CCM Buck converter has the lowest reliability degradation in the higher V_i levels. As V_i increases, the reliability performance of the DCM Buck–Boost and CCM Boost converter topologies will be negatively impacted the most.

In order to evaluate the effect of V_i on the failure rates of converter components, Figure 15(a) demonstrates the sensitivity of λ_S, λ_D, λ_L and λ_{Co} with respect to V_i in CCM operation. The sensitivities are assessed through$(d\lambda(V_i)/dV_i).(V_i/\lambda(V_i))$, where $\lambda(V_i)$ is replaced by$\lambda_S(V_i)$, $\lambda_D(V_i)$, $\lambda_L(V_i)$ and $\lambda_{Co}(V_i)$ for each component. As presented in Figure 15(a), the diodes in NIDC-DC converters are the most sensitive components to

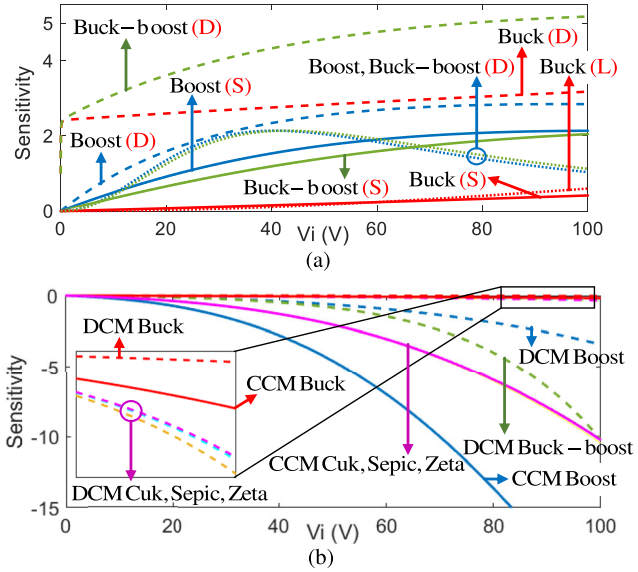

FIGURE 15 Sensitivity comparison of NIDC-DC converter topologies with respect to V_i at $t = 0.6 \times 10^6$ h: (a) Components' sensitivities in CCM operating mode; (b) Converters' overall sensitivities

V_i variations in all cases, where it takes the lead in the list in the case of the Buck–Boost converter. The analyses results, however, present that the switches are the most impactful elements on the overall reliability performance of the NIDC-DC converters. Note that the elements' sensitivity are almost similar in both CCM and DCM. Furthermore, the converters' overall reliability performance is compared in Figure 15(b), where the DCM Buck and CCM Boost converters are revealed to be the least and the most sensitive converter topologies. The sensitivity of the Cuk, Sepic and Zeta converters are similar in CCM, which is almost accurate in DCM operation, too. In addition, all the sensitivity factors in Figure 15(b) are found negative, reflecting the fact that the converters' reliability performance degrades as V_i increase—as also demonstrated in Figures 12, 13, and 14.

3.3 | Effects of output power and aging on reliability

The operating output power is one effective parameter on the reliability performance of power electronic converters. This section studies the effect of P_o variations on the reliability of the NIDC-DC converters in different t durations. Similar to the former analysis, the duty cycle in DCM and CCM operation modes are assumed 1/3 and 2/3, respectively. The components failure rates corresponding to the CCM Buck–Boost converter are determined as follows.

$$\lambda_{Co}(P_o) = 0.013\left(\left(5.12 \times 10^{-4} P_o^{1.5}\right) + 1\right) \tag{17}$$

$$\lambda_L(P_o) = 5 \times 10^{-5} \exp\left(-1276\left(\frac{1}{298 + 4.04P_o} - \frac{1}{298}\right)\right) \tag{18}$$

$$\lambda_S(P_o) = 0.48 \exp\left(-1925\left(\frac{1}{298 + 0.167P_o + 8.14\sqrt{P_o}} - \frac{1}{298}\right)\right) \tag{19}$$

$$\lambda_D(V_i) = 0.0038\left(\frac{P_o}{1568.47}\right)^{1.215} \times \exp\left(-3091\left(\frac{1}{298 + 0.045P_o + 10.88\sqrt{P_o}} - \frac{1}{298}\right)\right) \tag{20}$$

$$\lambda_{GD}(V_i) = 72 \times 10^{-6} \tag{21}$$

The reliability variations in the Buck and Buck–Boost converter topologies under both CCM and DCM operating modes are respectively illustrated in Figures 16 and 17, where the reliability performance is presented with respect to P_o and t. In addition, Figure 18 offers a precise reliability comparison among different classes of NIDC-DC converters from P_o perspective. The presented results demonstrate that the DCM operation is more reliable than CCM. Furthermore, reliability of Buck and Boost converters are the highest among the NIDC-DC converters when operated in the DCM, and this is the highest in the case of CCM for Buck converter. Such outstanding reliability performance in the Buck converter is owed to the comparatively lower value of λ_S with the highest effect on λ_{12}. In this converter, the switch is located in the lower current path, which tolerates less conduction loss. However, higher λ_S in Cuk, Sepic and Zeta converters causes their lower reliability value.

Figure 19(a,b) presents the sensitivities of λ_S, λ_D and λ_L of the NIDC-DC converters to P_o variations in DCM and CCM operations, respectively. The results reveal that λ_D, λ_L and λ_S are attributed the highest sensitivities in that order. Sensitivity of λ_L for CCM Boost and CCM Buck–Boost converters reaches a maximum value in 149 and 74 W, respectively. Furthermore, the sensitivity of switches in the CCM Boost and CCM Buck–Boost converters are found very similar, while λ_S in the Buck–Boost converter is more sensitive in DCM operating mode. The overall reliability sensitivity of different classes of NIDC-DC converters are compared in Figure 19(c). According to this figure, variations in P_o results in the lowest and highest impact on the DCM Boost and CCM Cuk converters, respectively. Negative sensitivity values in Figure 19(c) reflects the inverse proportion of reliability performance and P_o variations (as verified earlier).

3.4 | Effects of voltage gain and aging on reliability

The main role of NIDC-DC converters is changing the input voltage level to the desired voltage in the output port. In order

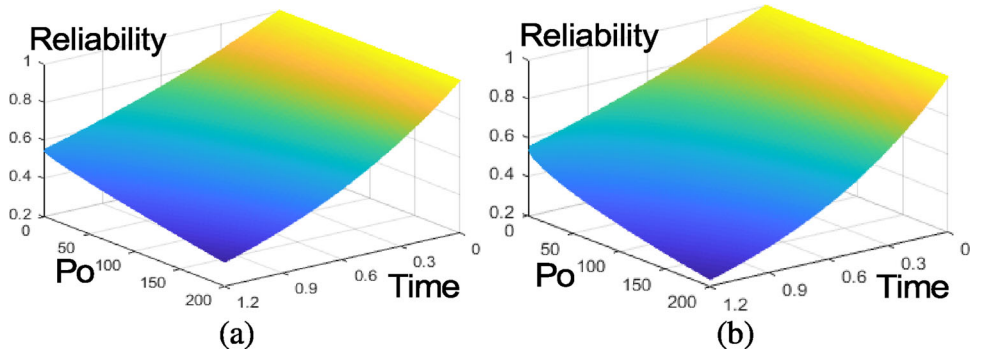

FIGURE 16 Reliability performance comparison with respect to P_o (W) and t (h×10^6): (a) DCM Buck; (b) CCM Buck

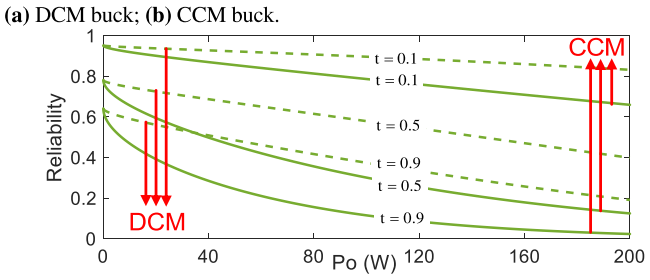

FIGURE 17 Reliability performance of the Buck–Boost converter with respect to P_o at different t (h×10^6)

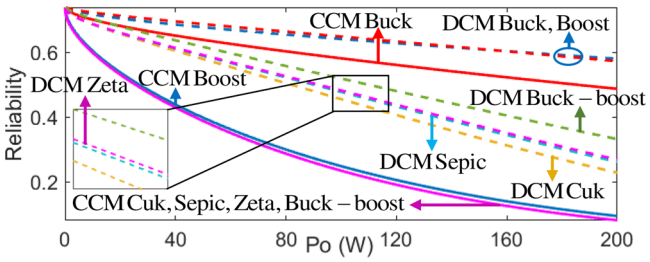

FIGURE 18 Reliability performance comparison of different NIDC-DC converter topologies with respect to P_o at $t = 0.6 \times 10^6$ h

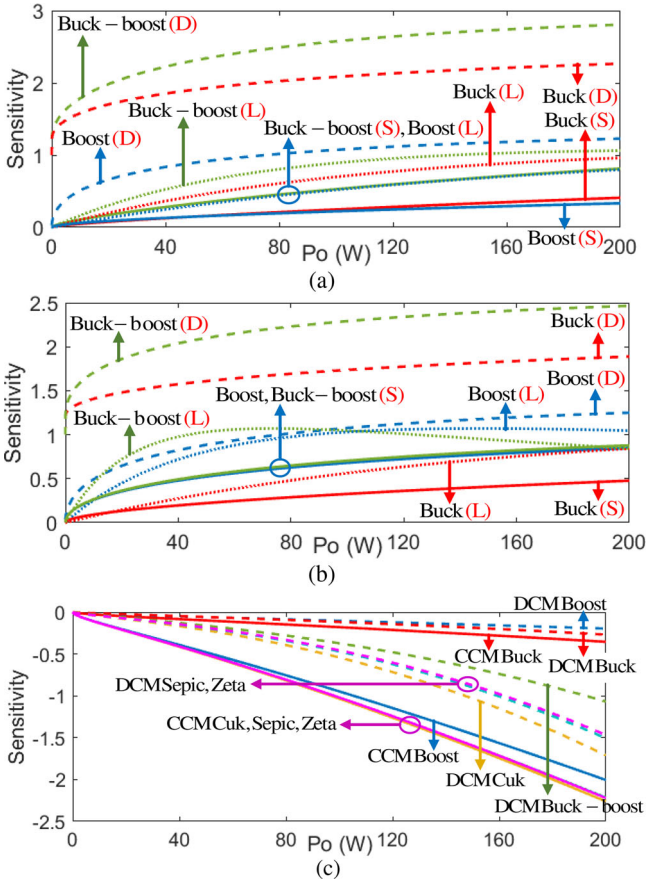

FIGURE 19 Sensitivity comparison of NIDC-DC converters with respect to P_o at $t = 0.6 \times 10^6$ h: Components sensitivities in (a) DCM and (b) CCM operating modes; (c) Converters' overall sensitivities

to reach the reliable operation, the reliability performance of NIDC-DC converters is evaluated with respect to G in this section. In Figure 20, a three-dimensional plot of the Buck–Boost converter reliability variation is depicted with respect to G and t, which verifies higher reliability of the Buck operation part ($G < 1$) than the Boost operation ($G > 1$). Moreover, reliability of other NIDC-DC converters are expressed in Figures 21 and 22. The precise comparison of reliability plots in this figure results that (i) much higher voltage gain leads to lower reliability, (ii) much lower voltage gain leads to lower reliability except the Boost converter, (iii) the Boost converter has higher reliability than the Buck–Boost and Cuk converters, since it operates with a lower duty cycle to reach a specific voltage gain, and (iv) $G = 0.47$, $G = 0.54$ and $G = 1$ have the highest reliability performance in Buck, Buck–Boost and Boost converters. Eventually, the reliability sensitivity of NIDC-DC converters is calculated and the results are shown in Figure 23, which validates the obtained results in Figures 21 and 22.

3.5 | Effects of components characteristics and aging on reliability

This section explores the power switch characteristics and how they affect the components failure rates and the overall

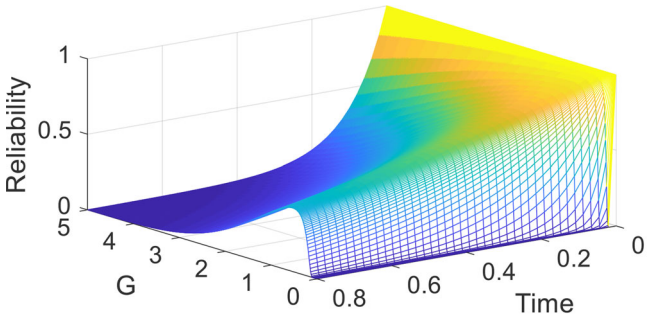

FIGURE 20 Reliability performance of the Buck–Boost converter with respect to G and t (h×10^6)

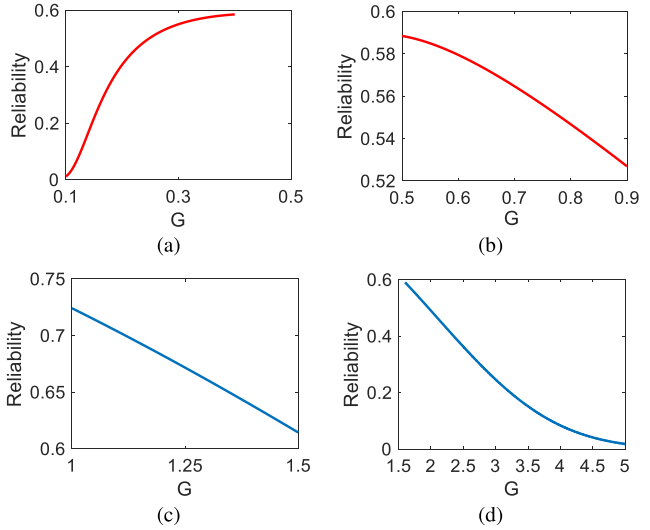

FIGURE 21 Reliability performance comparison of different NIDC-DC converter topologies with respect to G at $t = 0.6 \times 10^6$ h. (Part 1) (a, b) DCM and CCM Buck; (c, d) DCM and CCM Boost

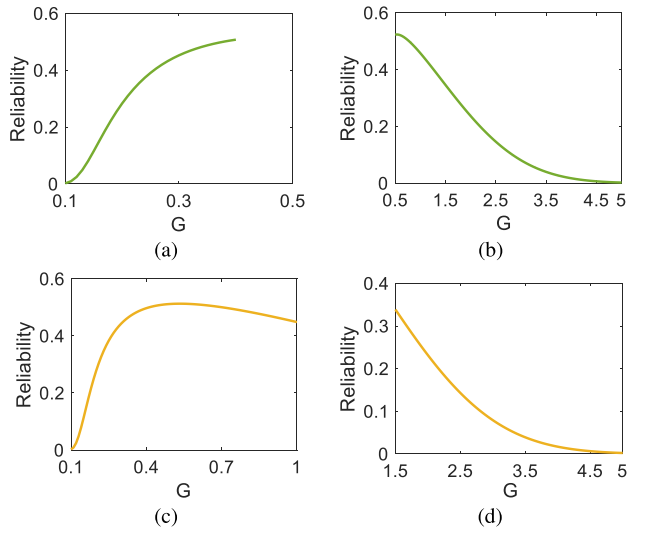

FIGURE 22 Reliability performance comparison of different NIDC-DC converter topologies with respect to G at $t = 0.6 \times 10^6$ h. (Part 2) (a, b) DCM and CCM Buck–Boost; (c, d) DCM and CCM Cuk

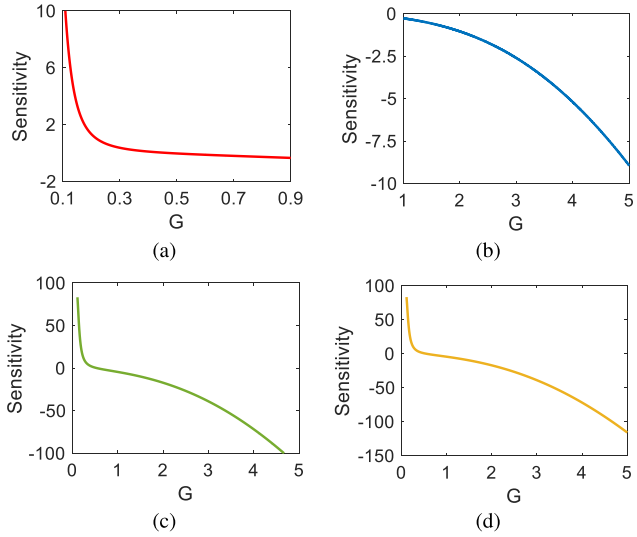

FIGURE 23 Sensitivity comparison of NIDC-DC converters with respect to G at $t = 0.6 \times 10^6$ h: (a) Buck. (b) Boost; (c) Buck–Boost; (d) Cuk

TABLE 2 Important characteristics of selected power switches for reliability assessment

	IRFPxxxxPbF Power MOSFETs					
Parameters	**4242**	**4232**	**4229**	**4137**	**4668**	**4868**
V_{DS} (V)	360	300	300	300	200	300
R_{DS} (mΩ)	49	30	38	56	8	25.5
C_{oss} (pF)	520	610	390	300	810	612
$T_{d(on)}$ (ns)	40	37	25	18	41	24
$T_{d(off)}$ (ns)	72	64	44	34	64	62

reliability performance of NIDC-DC converters. Several number of representative switches are selected with the corresponding λ_S calculated for different classes of NIDC-DC converters in CCM and DCM. Table 2 presents the important characteristics of a family of power MOSFETs (IRFP4xxxPbF) which are assorted into two categories; effective on conduction loss or switching loss. Drain-source ON-resistance (R_{DS}) is a critical parameter characterizing the conduction loss of a switch. The turn-on delay time ($T_{d(on)}$), turn-off delay time ($T_{d(off)}$) and the output capacitance (C_{oss}) are critical parameters in the switching loss assessments. Moreover, drain-source breakdown voltage (V_{DS}) represents the tolerable voltage across the switch. Failure rates for different switches under the same operating conditions for NIDC-DC converters are assessed as tabulated in Table 3, where $P_o = 100$Wand the duty cycles are $D = 1/3$ and $D = 2/3$ in DCM and CCM, respectively. Comparing the results in Table 2 and Table 3, one can clearly realize how each of the critical parameters play a role onλ_S. Additionally, the evaluation results do not reveal a particular pattern, when considering all the critical parameters, in assessingλ_S. Hence, the set of critical parameters should be taken into account along with the converters' operational characteristics to conclude about the failure

TABLE 3 Assessed failure rates of selected power switches

Converters		IRFPxxxxPbF Power MOSFETs					
		4242	4232	4229	4137	4668	4868
CCM	Buck	0.92	0.92	1.03	1.02	1.08	1.05
	Boost	2.31	2.18	2.99	3.11	2.77	2.87
	Buck–Boost	2.38	2.27	3.04	3.16	2.89	3.00
	Cuk, Sepic, Zeta	2.38	2.27	3.04	3.16	2.89	3.00
DCM	Buck	0.69	0.77	0.65	0.58	1.02	0.83
	Boost	0.47	0.47	0.57	0.57	0.59	0.59
	Buck–Boost	1.02	1.09	1.03	0.96	1.40	1.23
	Cuk, Sepic, Zeta	1.08	1.11	1.19	1.16	1.39	1.30

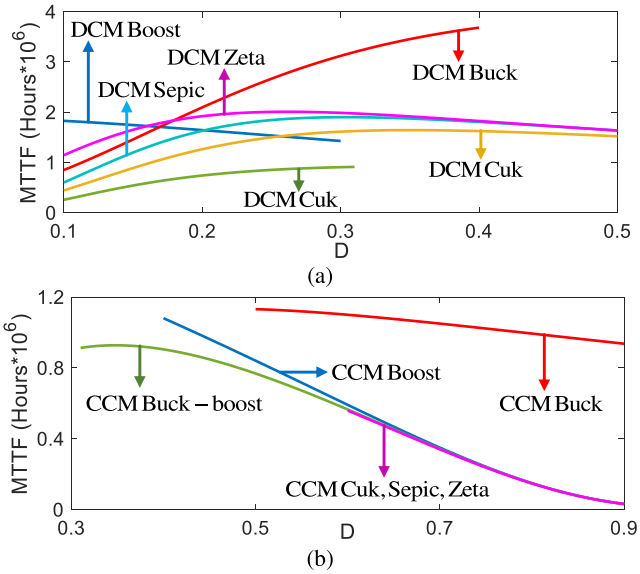

FIGURE 24 (Part 1) Converters' MTTF comparison with respect to: (a) D in DCM; (b) D in CCM

rates in different scenarios. For instance, (i) high values of C_{oss} and $T_{d(on)}$ in IRFP4868 when V_{DS} and R_{DS} remain low result in the highest λ_S in most NIDC-DC converter topologies; (ii) high conduction loss in IRFP4137 ($R_{DS} = 56\,\Omega$) is more influential on the failure rate than its low switching losses ($T_{d(on)}$, $T_{d(off)}$ and C_{oss}); and (iii) higher V_{DS} in IRFP4242 compensates the conflictive effect of $T_{d(off)}$.

4 | MTTF ANALYSIS RESULTS

Complementary to the proposed reliability analytics and failure rate analysis of different classes of NIDC-DC converters, this section is devoted to MTTF evaluations as discussed earlier in Equation (6). Figures 24(a) and 25(b) respectively demonstrate the MTTF results for NIDC-DC converters in DCM and CCM

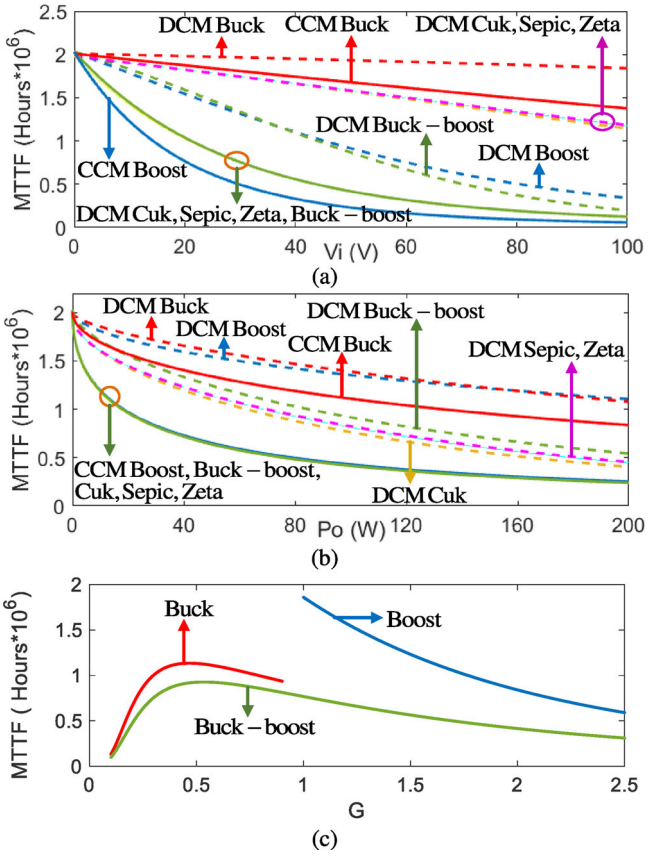

FIGURE 25 (Part 2) Converters' MTTF comparison with respect to: (a) V_i; (b) P_o; and (c) G

with respect to variations in D. One can see from Figures 24 and 25 that the Buck converter is found to have the highest MTTF values (with the exceptional interval of $D < 0.17$), while the DCM Boost converter topology operates as the most reliable. The MTTF results confirms the previous evaluations illustrated in Figure 9. In Figure 25(a), the MTTF values are presented in different V_i values, in which the DCM Buck, CCM Buck and DCM Cuk, Sepic and Zeta converter topologies are attributed the highest MTTF in that order, while CCM Boost converter reveals the lowest MTTF. Such observations are in full agreement with those of Figure 14. In Figure 25(b), the MTTF is presented with respect to the output power, where the DCM Buck, DCM Boost and CCM Buck show the highest MTTF, validating the results previously reported in Figure 18. Finally, Figure 25(c) presents the MTTF with respect to G variation.

5 | EXPERIMENTAL VERIFICATION AND THERMAL TESTS

Figure 26 demonstrates the experimental setups of the Buck and Boost converters with the same design characteristics studied in the theoretical analyses of this paper, where the corresponding components of the schematic view and experimental setups are identified with the same alphabetic letters. These two NIDC-DC converter topologies are representatively selected to assess

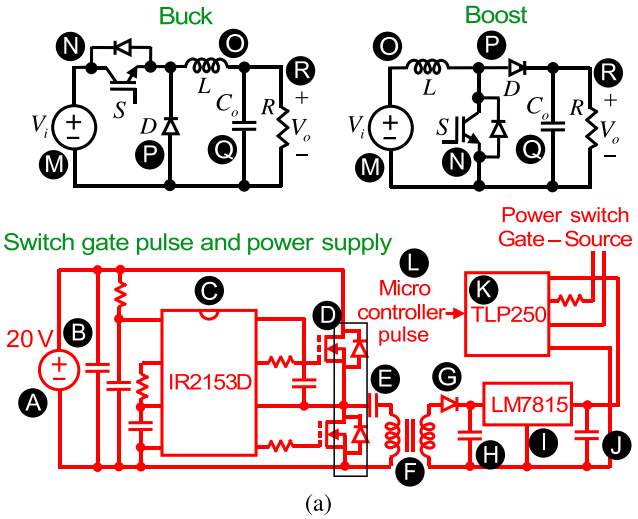

(a)

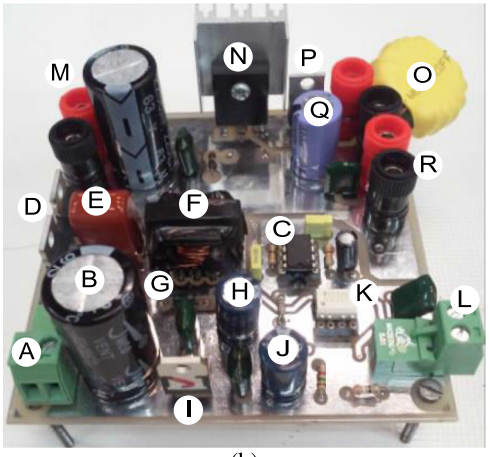

(b)

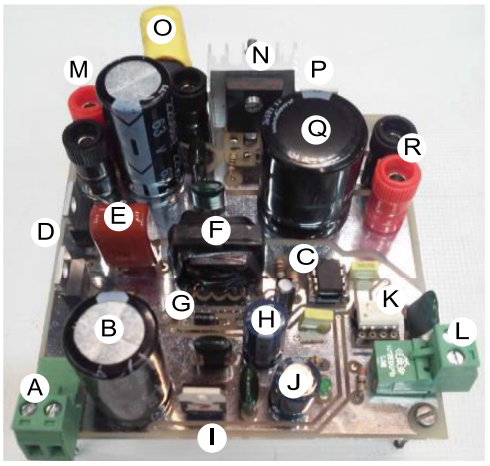

(c)

FIGURE 26 Experimental prototypes of converters: (a) Schematic view of converters, device power supply and gate driver; (b) Buck; (c) Boost

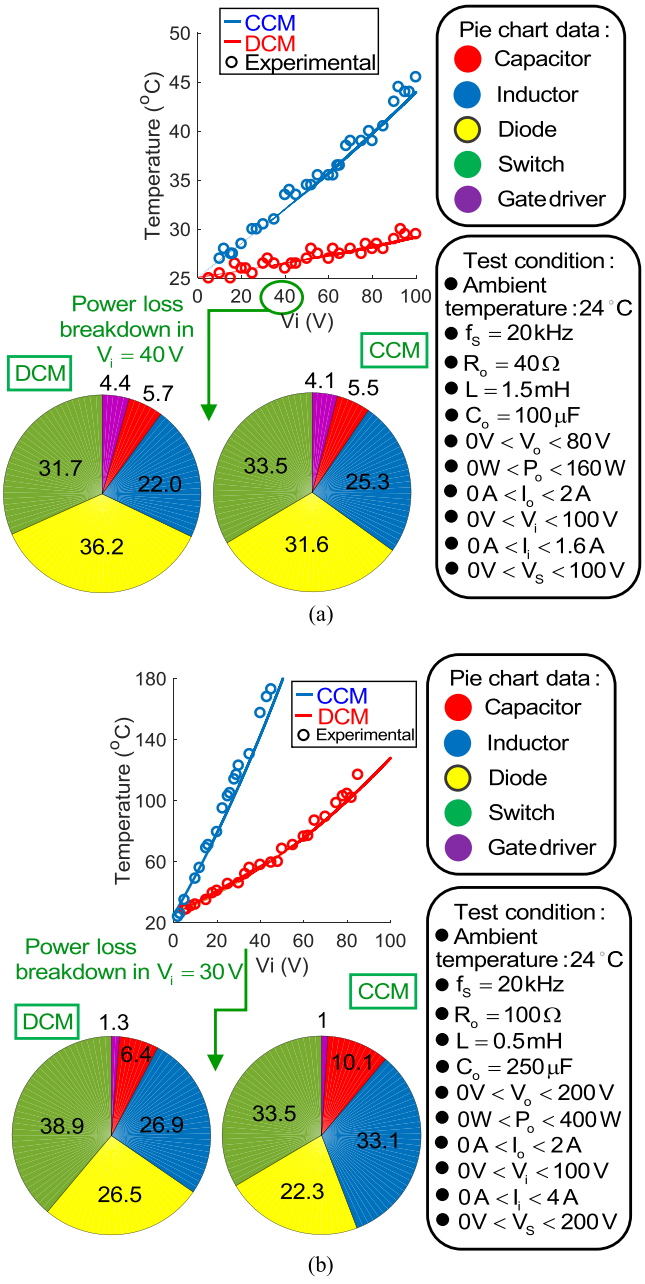

FIGURE 27 (Part 1) Experimental and theoretical temperature and power loss test results for the power switch in different operational conditions with respect to V_i in (a) Buck converter, (b) Boost converter

their thermal performance (reflected through temperature variations) in different operational conditions and under numerous tests. While the temperature values of all power circuit components are measured and recorded through the experiments, the results are presented only for the switch elements as they demonstrated a critical role on the converter's reliability performance. The thermal test results on the Buck and Boost converters and the obtained power loss breakdown charts are plotted in Figures 27, 28 and 29 with respect to V_i, P_o and D in both DCM and CCM operation modes. As one can see from the presented results in Figures 27, 28 and 29, the experimental observations closely follow the theoretical analyses, further verifying the accuracy and effectiveness of the suggested analytics for reliability evaluation of NIDC-DC converters. Note that the small differences between the theoretical and experimental observations are primarily driven by factors such as the interstitial heat radiation of components, measurement accuracy, and ambient

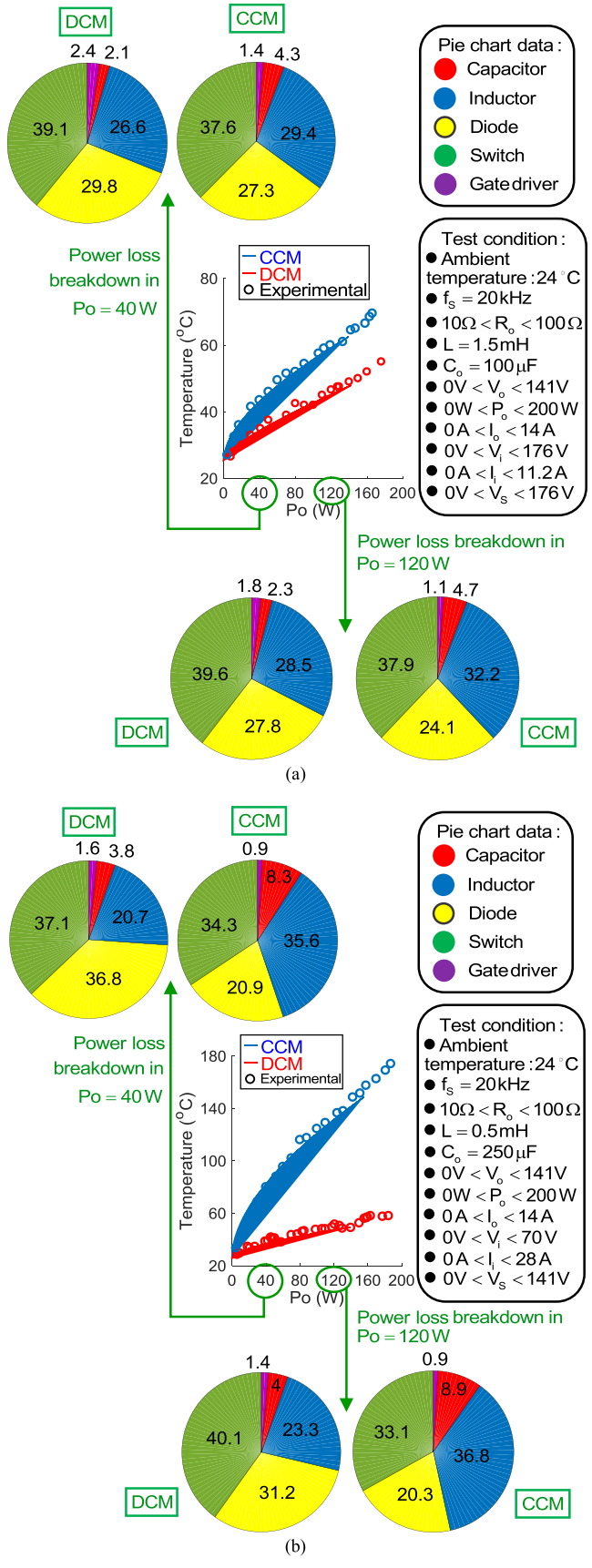

FIGURE 28 (Part 2) Experimental and theoretical temperature and power loss test results for the power switch in different operational conditions with respect to P_o in (a) Buck converter, (b) Boost converter

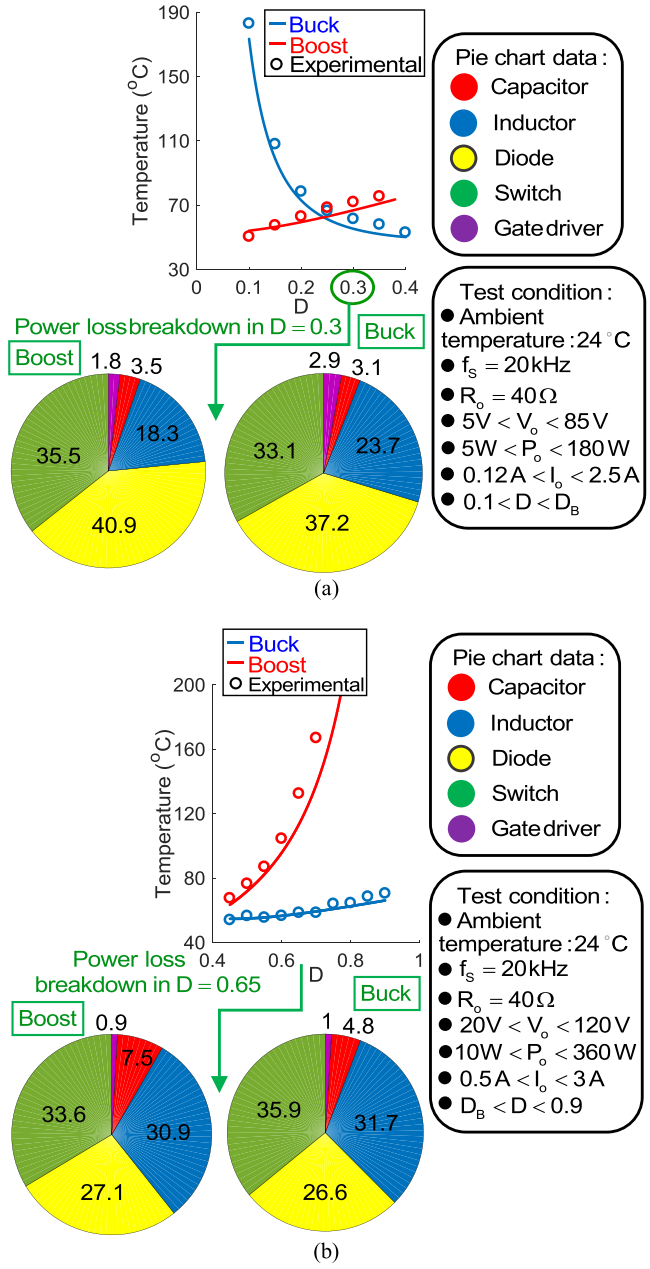

FIGURE 29 (Part 3) Experimental and theoretical temperature and power loss test results for the power switch in different operational conditions with respect to: *D* in (a) DCM, (b) CCM

temperature changes. In addition, some selected thermo-vision examples of the experimental prototypes are illustrated in Figure 30 (the Buck converter) and Figure 31 (the Boost converter), in which the coldest (ambient) and hottest (switch) points are determined.

6 | CONCLUSION

In this paper, a holistic framework for reliability assessment of NIDC-DC converters is proposed that, different from the state-of-the-art literature, can effectively capture the effects of

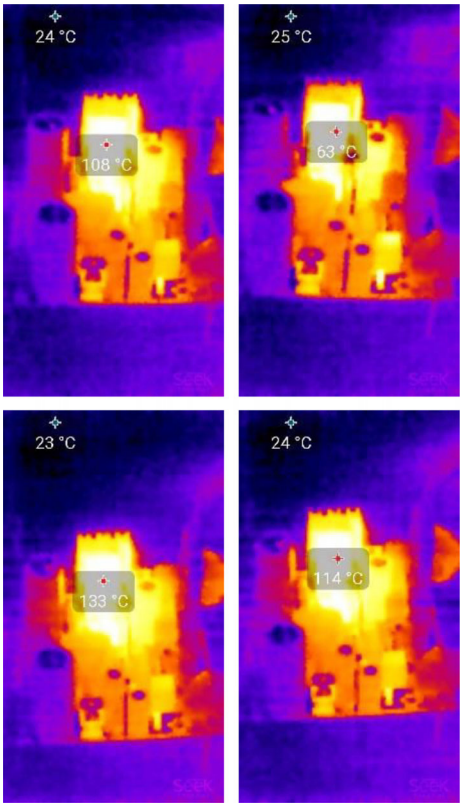

FIGURE 30 Sample thermo-vision demonstrations of the Buck converter experimental prototype

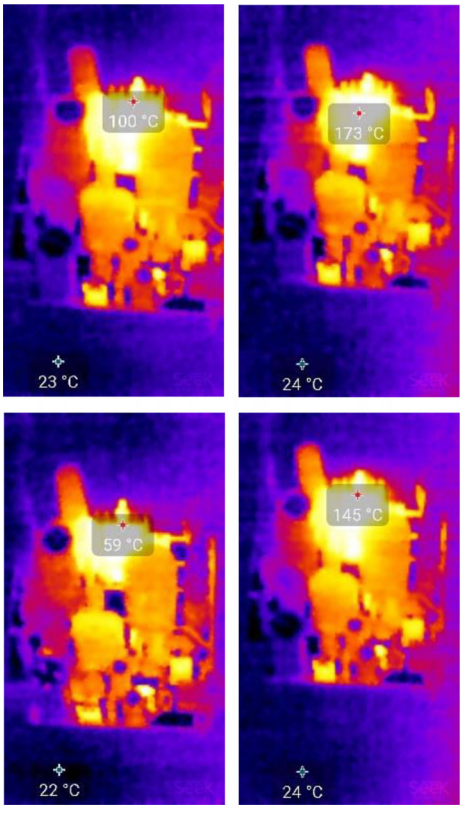

FIGURE 31 Sample thermo-vision demonstrations of the Boost converter experimental prototype

various contradictory characteristics and operating conditions, e.g. duty cycle, input voltage, output power, components characteristics and aging. Extensive sensitivity analyses were performed to understand how sensitive the converters' reliability performance and the components' failure rates are to changes in critical parameters. Centred on the Markov process, the MTTF index of reliability was evaluated under different duty cycles, input voltages and output power values, the observations on which were primarily in line with the proposed analytics. Supported by experimental tests and thermal assessments, it was concluded that, under the same operating conditions, the DCM operation of NIDC-DC converters generally results in a higher MTTF and reliability performance than that under CCM. Additionally, the Buck converter topology was revealed to be most reliable among different classes of NIDC-DC converters in both DCM and CCM. Eventually, it was demonstrated that failure rates of the switches play a significant role on the converters' overall reliability performance.

ACKNOWLEDGMENTS

The authors would like to sincerely thank Prof. Mehdi Fardmanesh and Dr. Seyed Iman Mirzaie (Superconductor Electronics Research Lab., Sharif University of Technology) for their cooperation in the experimental tests.

REFERENCES

1. Azadeh, Y., et al.: Single-inductor dual-output DC–DC converter with capability of feeding a constant power load in open-loop manner. IEEE Trans. Ind. Electron. 66(9), 6906–6915 (2019)
2. Tarzamni, H., et al.: High step-Up DC-DC converter with efficient inductive utilization. IEEE Trans. Ind. Electrons. 1–1 (2020, in press). https://doi.org/10.1109/TIE.2020.2987253
3. Kolahian, P., et al.: Multi-port DC–DC converter for bipolar medium voltage DC micro-grid applications. IET Power Electron. 12(7), 1841–1849 (2019)
4. Richardeau, F., Pham, T.T.L.: Reliability calculation of multilevel converters: theory and applications. IEEE Trans. Ind. Electron. 60(10), 4225–4233 (2013)
5. Tarzamni, H., et al.: Analysis and reliability evaluation of a high step-up soft switching push–pull DC–DC converter. IEEE Trans. Reliability 1–11 (2019, in press)
6. Tarzamni, H., et al.: Reliability analysis of buck-boost converter considering the effects of operational factors. In: The International Power Electronics, Drive Systems and Technologies Conference (PEDSTC). Shiraz, Iran, pp. 647–652 (2019)
7. Zhou, D., et al.: Comparison of wind power converter reliability with low-speed and medium-speed permanent-magnet synchronous generators. IEEE Trans. Ind. Electron. 62(10), 6575–6584 (2015)
8. Jahan, H.K., et al.: Low component merged cells cascaded-transformer multi-level inverter featuring an enhanced reliability. IET Power Electron. 10(8), 855–862 (2017)
9. Zhou, D., et al.: Mission profile based system-level reliability analysis of DC/DC converters for a backup power application. IEEE Trans. Power Electron. 33(9), 8030–8039 (2018, in press)
10. Alam, M.K., Khan, F.H.: Reliability analysis and performance degradation of a boost converter. IEEE Trans. Ind. Appl. 50(6), 3986–3994 (2014)
11. Liu, Y., et al.: Reliability-oriented optimization of the LC filter in a buck DC-DC converter. IEEE Trans. Power Electron. 32(8), 6323–6337 (2017)
12. Rahimi, T., et al.: Three-phase soft-switching-based interleaved boost converter with high reliability. IET Power Electron. 10(3), 377–386 (2017)

13. Hsieh, Y.C., et al.: An interleaved boost converter with zero-voltage transition. IEEE Trans. Power Electron. 24(4), 973–978 (2009)
14. Jain, N., et al.: A zero voltage transition boost Converter employing a soft switching auxiliary circuit with reduced conduction losses. IEEE Trans. Power Electron. 19(1), 130–139 (2004)
15. Aghdam, F.H., Abapour, M.: Reliability and cost analysis of multistage boost converters connected to PV panels. IEEE J. Photovoltaics 6(4), 981–989 (2016)
16. Khosroshahi, A., et al.: Reliability evaluation of conventional and interleaved DC–DC boost converters. IEEE Tran. Power Electron. 30(10), 5821–5828 (2015)
17. Dhople, S.V., et al.: A unified approach to reliability assessment of multiphase DC–DC converters in photovoltaic energy conversion systems. IEEE Trans. Power Electron. 27(2), 739–751 (2012)
18. Tarzamni, H., et al.: Interleaved full ZVZCS DC–DC boost converter: analysis, design, reliability evaluations and experimental results. IET Power Electron., 10(7), 835–845 (2017)
19. Pei, X., et al.: Open-circuit fault diagnosis and fault-tolerant strategies for full-bridge DC–DC converters. IEEE Trans. Power Electron. 27(5), 2550–2565 (2012)
20. Jamshidpour, E., et al.: Single-switch DC–DC converter with fault-tolerant capability under open- and short-circuit switch failures. IEEE Trans. Power Electron. 30(5), 2703–2712 (2015)
21. Tarzamni, H., et al.: Comprehensive analytics for reliability evaluation of conventional isolated multiswitch PWM DC–DC converters. IEEE Trans. Power Electron. 35(5), 5254–5266 (2020)
22. Reliability prediction of electronic equipments. Rep. MIL-HDBK-217. Relex Software Corp., Greensburg, Pennsylvania (1990)
23. Reliability Prediction Models. Reliability Information Analysis Center, 6000 Flanagan Rd, Suite 3, Utica, NY 13502-1348, RIAC-MIL-HDBK-217Plus, (2006)
24. Billinton, R., Allan, R.N.: Reliability Evaluation of Enginearing Systems, Concepts and Techniques. 2nd ed., pp. 260–306. Springer Scince+Business Media Press, New York (1992)
25. Kazimierczuk, M.K.: Pulse-width Modulated DC-DC Power Converters. pp. 139–188. Wiley, Hoboken, New Jersey (2008)

How to cite this article: Tarzamni H, Esmaeelnia FP, Tahami F, et al. Thermal analysis of non-isolated conventional PWM-based DC–DC converters with reliability consideration. *IET Power Electron.* 2021;14:337–351. https://doi.org/10.1049/pel2.12037